Sedimentology (1996) **43**, 973–993

Extensive carbonate algal bioherms in upper Pleistocene saline lakes of the central Altiplano of Bolivia

JEAN MARIE ROUCHY,* MICHEL SERVANT,† MARC FOURNIER† and CHRISTIANE CAUSSE*
**CNRS-UA 723, Laboratoire de Géologie, Muséum National d'Histoire Naturelle, 43, rue Buffon, 75005 Paris, France (E-mail: rouchy@mnhn.fr)*
†ORSTOM, Centre de Bondy, 72, rue d'Aulnay, 93143 Bondy cedex, France

ABSTRACT

During the upper Pleistocene the Central Altiplano of Bolivia was repeatedly flooded by deep and extensive saline lakes in response to climatic fluctuations. Development of carbonate algal bioherms took place during at least three major periods of lacustrine highstands, discontinuously covering the 300-km-long and 100-km-wide lacustrine slopes and terraces up to an elevation of 100 m above the surface of the modern halite crust of Uyuni. Distribution, size and shape of the bioherms are diverse due to various factors, e.g. the nature and morphology of the substrate and the hydrodynamic conditions that prevailed during growth. On larger palaeoterraces, the build-ups coalesced to form platform-like carbonate accumulations. Although the morphologies closely resemble those induced by cyanobacteria, they were predominantly constructed by other plant communities, probably dominated by filamentous green algae. Cyanobacterial communities flourished in association with these plants, but they did not contribute significantly to the architecture of the bioherms; they participated to encrust the plant stems and algal bushes or to form thin laminated layers covering the build-ups. A prominent feature of some bioherms is their composite structure due to repeated algal growth during successive lacustrine episodes that were separated by subaerial exposures with moderate erosional effects. The build-ups located between 3660 and 3680 m elevation display up to three major parts: (1) a massive inner core formed during an early Minchin highstand, before 40 ka; (2) a large peripheral envelope deposited at about 40 ka (late Minchin) and (3) a thinner outermost crust formed during a late glacial event. Lake level dropped during interlacustrine stages, sometimes leading to desiccation and deposition of salt layers in the deepest parts of the system, i.e. the present-day salar of Uyuni.

INTRODUCTION

The development of fresh-water carbonate algal bioherms involves the activity of various plants and organisms. However, most of the algal carbonates reported in modern settings are predominantly formed by the activity of cyanobacterial communities producing diverse stromatolitic build-ups (Dean & Eggleston, 1975; Eggleston & Dean, 1976; Dean & Fouch, 1983; Moore *et al.*, 1984; Cohen & Thouin, 1987; Kempe *et al.*, 1991; Winsborough *et al.*, 1994; Casanova, 1986, 1992, 1994). Large tufa pinnacles mostly of algal origin were formed during the Quaternary in some lacustrine systems of the south-western United States (Scholl, 1960; Scholl & Taft, 1964; Benson, 1994, 1995). Tubes of phrygan larvae encrusted by algae may have also contributed to form the frame of large carbonate build-ups in Oligocene deposits of France (Freytet & Plaziat, 1965, 1982; Bertrand-Sarfati *et al.*, 1966, 1994). The Miocene deposits of the Ries Crater lake (Germany) provide the only

known occurrence of large mounds built by the green alga *Cladophorites* (Riding, 1979).

The central and southern part of the Bolivian Altiplano shows an unusual development of carbonate algal bioherms plastering the palaeoslopes of lakes which repeatedly flooded this area during the Late Pleistocene. The extent and depth of these palaeolakes changed greatly according to variations in the rainfall/evaporation rate (Hastenrath & Kutzbach, 1985; Servant *et al.*, 1995).

The carbonate bioherms exhibit various morphologies similar to those of stromatolites although the frame of the build-ups was formed predominantly by different plant assemblages mainly composed of green algal microflora, with associated cyanobacterial communities. By comparison with other occurrences reported in the literature the algal bioherms of the central Altiplano present an unusually extensive development inasmuch as they can be observed discontinuously over more than 300 km from north to south and locally across 100 km. Moreover, these bioherms display an uncommon example of composite build-up morphology caused by periods of repeated algal colonization during successive lacustrine highstands, providing an accurate record of the fluctuations of the upper Pleistocene lake. During lowstands, the lake level dropped, leading to the deposition of salt layers in the deepest parts of the basin which correspond to the salar of Uyuni.

This paper deals with one of the more extensive sequences of lacustrine algal constructions from a part of the world which is poorly known. The purpose is to document the distribution of the bioherms according to the basin configuration and elevational fluctuations of the lake, the composition of the algal builders, the organization of the build-ups and their sequence of construction. In addition, this study provides a new chronology of the lake-level variations necessary to refine our understanding of the regional climate.

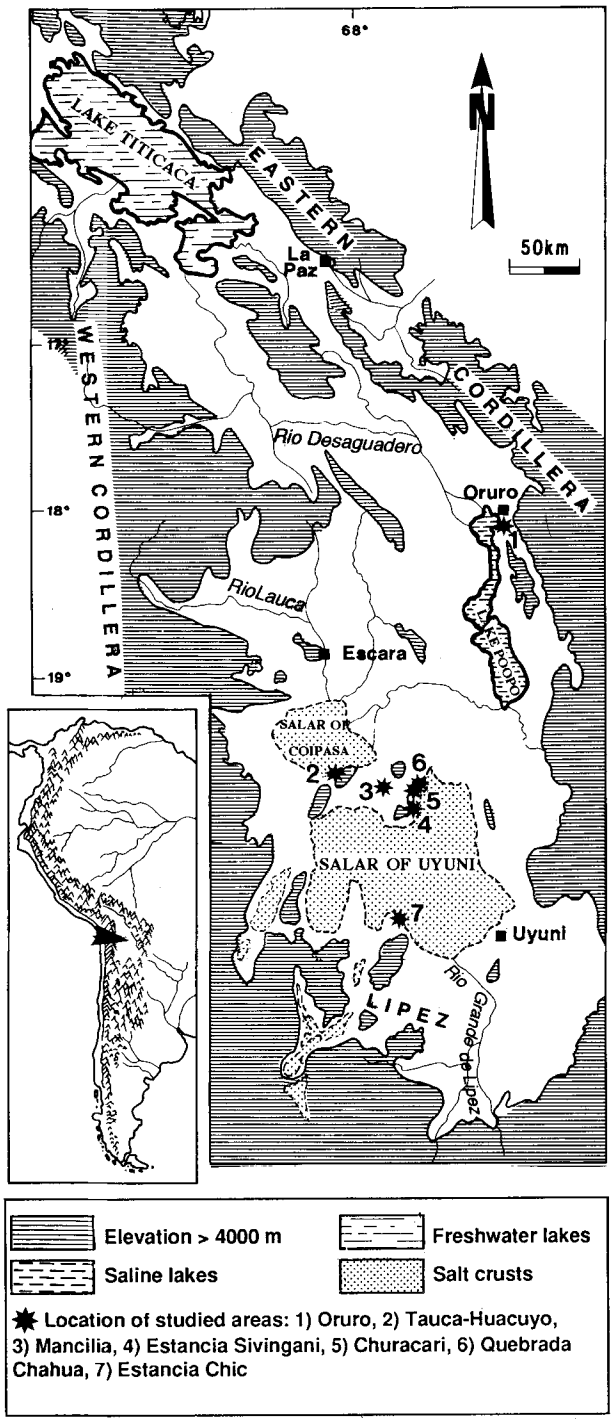

Fig. 1. Sketch map of the Bolivian Altiplano with the distribution of the main lacustrine systems and the location of the studied sites.

GEOLOGICAL AND HYDROLOGICAL BACKGROUND

The Altiplano of Bolivia is a gently dipping high plateau about 1000 km long and 200 km wide with elevation ranging from 3653 m at the surface of the Uyuni salt crust to about 4600 m in the southernmost Lipez area (Fig. 1). It constitutes a large intermontane endoreic system enclosed between two highly deformed orogenic ranges, i.e. the Eastern Cordillera and the Western Cordillera which rise locally up to 6500 m.

The regional climate displays a strong NE–SW gradient of temperature and rainfall with annual mean values of 15°C and 700 mm in the north to 7°C and 100 mm in the south (Lipez), where the

Table 1. Chronology of the main lacustrine episodes.

Main lacustrine highstands	Conventional ^{14}C ages		U/Th ages		Maximum elevations
	Rondeau (1990)*	Servant *et al.* (1995)†	Rondeau (1990) (1)*	Causse *et al.* (1995) (2)*	
Coipasa	7·9–9·85 ka BP	10·4–11·3 ka BP	Third generation		3660 m
(*Ticana lowstand*)	Third generation	11·9–15·4 ka BP (highest level: 12–13 ka BP)		15·07–16·2 ka (highest level; 15·07 ka)	
Tauca	11–14·1 ka BP		7–14·8 ka		3750–3760 m
Upper Minchin	Second generation ‡8·8–30·8 ka BP	27 ka BP	Second generation 34–44 ka	*c.* 40 ka	3730 m ?
Lower Minchin	First generation >26·2–34·2 ka BP		First generation 68–72·5 ka		3660–3680 m (Estancia Sivingani Estancia Chic) 3705 m (Oruro)

Episodes names from Servant & Fontes (1978) and Servant *et al.* (1995). (1) Alpha spectrometry dates; (2) TIMS dates. *Ages obtained on carbonate build-ups. †Ages obtained on lacustrine deposits (*Chara*, shells, aragonitic layers). ‡Apparent ages (bulk carbonates).

winter temperature may drop to –30°C (Servant & Fontes, 1978; Risacher, 1978, 1992). The average evaporation rate ranges between 1500 and 2000 mm yr^{-1}.

According to both morphological and climatic characteristics, the Altiplano displays different hydrological settings (Fig. 1). The northern Altiplano is occupied by the freshwater Lake Titicaca (salinity less than 1 g L^{-1}) which drains southward into Lake Poopo through the Desaguadero river. The endoreic system of the central altiplano comprises three sub-basins located at different elevations: (1) the northern sub-basin with lake Poopo (3686 m) – mean salinity about 30 g L^{-1} (Risacher, 1992); (2) the central sub-basin with the salar of Coipasa (3657 m) covered by a large salt crust (about 2500 km^2) with a restricted shallow sheet of hypersaline waters and (3) the southern sub-basin including the salar of Uyuni (3653 m) covered by the largest salt crust in the world (10 000 km^2). The southern Altiplano (Lipez area) contains a lot of smaller hypersaline lakes and dry playas.

The Quaternary sedimentary successions reveal three main lacustrine highstands formerly named the Tauca, Minchin and Escara episodes (Servant & Fontes, 1978). Rondeau (1990) was the first to provide a description of the bioherms (interpreted as stromatolites) found in these lacustrine episodes and a chronological framework by U/Th and radiocarbon dating of three main generations of stromatolites (Table 1). This preliminary chronology has been refined by new ^{14}C and U/Th dating (Causse *et al.*, 1995; Servant *et al.*, 1995). Table 1 shows that, during the youngest episode (Late Glacial stage), the lake level culminated between 13 and 12 ^{14}C ka BP or 15 ka (U/Th) (Tauca event). After this maximum stand, it dropped abruptly until 11·4 ^{14}C ka BP (Ticana event) and then remained low, except for a small positive oscillation between 11·4 and 10·4 ^{14}C ka BP (Coipasa event). The upper Minchin event occurred around 40 ka (U/Th date), but further dating is needed to constrain the chronology of the pre-Tauca episodes, taking into account the different growth stages of the carbonate build-ups identified in this paper.

In the Lipez area, small isolated and perched saline lakes developed during the Tauca and Minchin episodes (Servant-Vildary & Mello e Sousa, 1993). Algal carbonate constructions are locally present along the palaeoslopes of some of these lakes while large pisoliths are formed in the Laguna Pastos Grandes within pools fed by hot springs (Risacher & Eugster, 1979; Jones & Renaut, 1994).

Widespread salt deposition took place during the interlacustrine stages in the Uyuni depression where 11 halite units 3–20 m in thickness have been recovered in a 121-m-long drill core

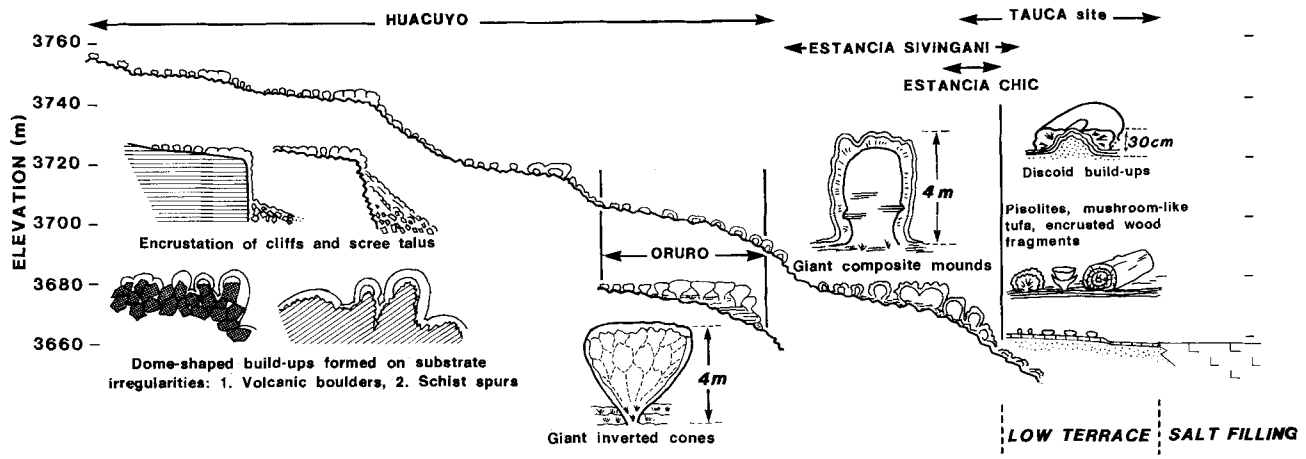

Fig. 2. Schematic distribution of the various types of algal carbonate bioherms according to the palaeotopography of the lacustrine palaeoslopes, with indication of the main studied sites.

(Risacher, 1992). The uppermost layer in this core (about 10 m thick) could have resulted from desiccation of lake Tauca (Risacher & Fritz, 1991).

DISTRIBUTION OF THE ALGAL BIOHERMS

Several localities were selected for detailed observations and sampling of the carbonate build-ups, i.e. Estancia Sivingani (3660–3670 m), Estancia Chic (3660–3670 m), Oruro (3700 and 3720 m), Churacari (3680 m), Mancilia (3700–3750 m) and Tauca-Huacayo (3660–3750/3760 m) (Fig. 1). They provide a significant survey of the various types of algal build-ups which plastered the outcropping palaeoslopes in the three main subbasins, from the Uyuni salt crust (3653 m) to the highest build-ups located near 3750/3760 m (Fig. 2). The uppermost build-ups appear as scattered fragments, suggesting their presence is limited by erosion. It is likely that algal bioherms are also present on buried palaeoslopes under the Uyuni salt crust.

Rondeau (1990) reported that the carbonate deposits were preferentially developed on three main terraces, i.e. 3700, 3720 and 3742 m. However, new field observations and altitude measurements show that the carbonate build-ups are present on four major erosional terraces, near 3660–3670, 3700, 3720 and 3745 m, as well as on smaller ones at 3730 and 3750/3760 m (Figs 2 and 3A–D). These terraces may form either gently inclined surfaces dissected by erosion into large headlands pointing lakeward (Fig. 3D) or narrow stairs in a chaotic accumulation of volcanic boulders (Fig. 3C). On wider terraces, both density and height of build-ups increase up to the break of slope, forming small carbonate platforms or reef-like lenses composed of aggregated domes (Fig. 3D). Progradational features are common (Fig. 3D) and the upper parts of the domes are usually truncated by an erosion surface. Thinner carbonate crusts are seen covering many kinds of morphologies including vertical palaeocliffs (Fig. 3E) or steep scree talus (Fig. 3F). Different types of smaller build-ups and carbonate crusts (Fig. 2) are observed on the marginal flats ('low-terrace') that surround the salars of Coipasa and Uyuni (3653–3657 m).

The algal bioherms display variable sizes, shapes and organization according to their age, location on palaeotopography, hydrological

Fig. 3. Relationships of the carbonate build-ups to the morphology of the lacustrine palaeoslopes. (A) Aggregates of algal build-ups on the terrace at 3740 m showing reef-like pattern with encrustation of the terrace palaeoslope (arrows). Huacuyo. Scale bar is ~10 m. (B) Algal build-ups covering the terrace at 3740 m in front of the salar of Coipasa (S). Huacuyo. The approximate height of the buildups is 1·5 m. (C) Carbonate-cemented erosional steps (arrows) in volcanic boulder accumulations. The top of the section corresponds to the platform of the terrace at 3740 m. Mancilia. Scale bar=10 m. (D) Algal carbonate platform composed of giant composite bioherms developed on a large erosional headland that extends lakeward (terrace at 3660–3680 m). Estancia Sivingani. The length of the platform is about 500 m and its maximum height 8 m. (E) Carbonate cemented palaeocliff on the terrace break of slope. 3680 m. Quebrada Chahua. Scale bar=1 m. (F) Carbonate-cemented steep scree talus. Mancilia. Scale bar=2 m.

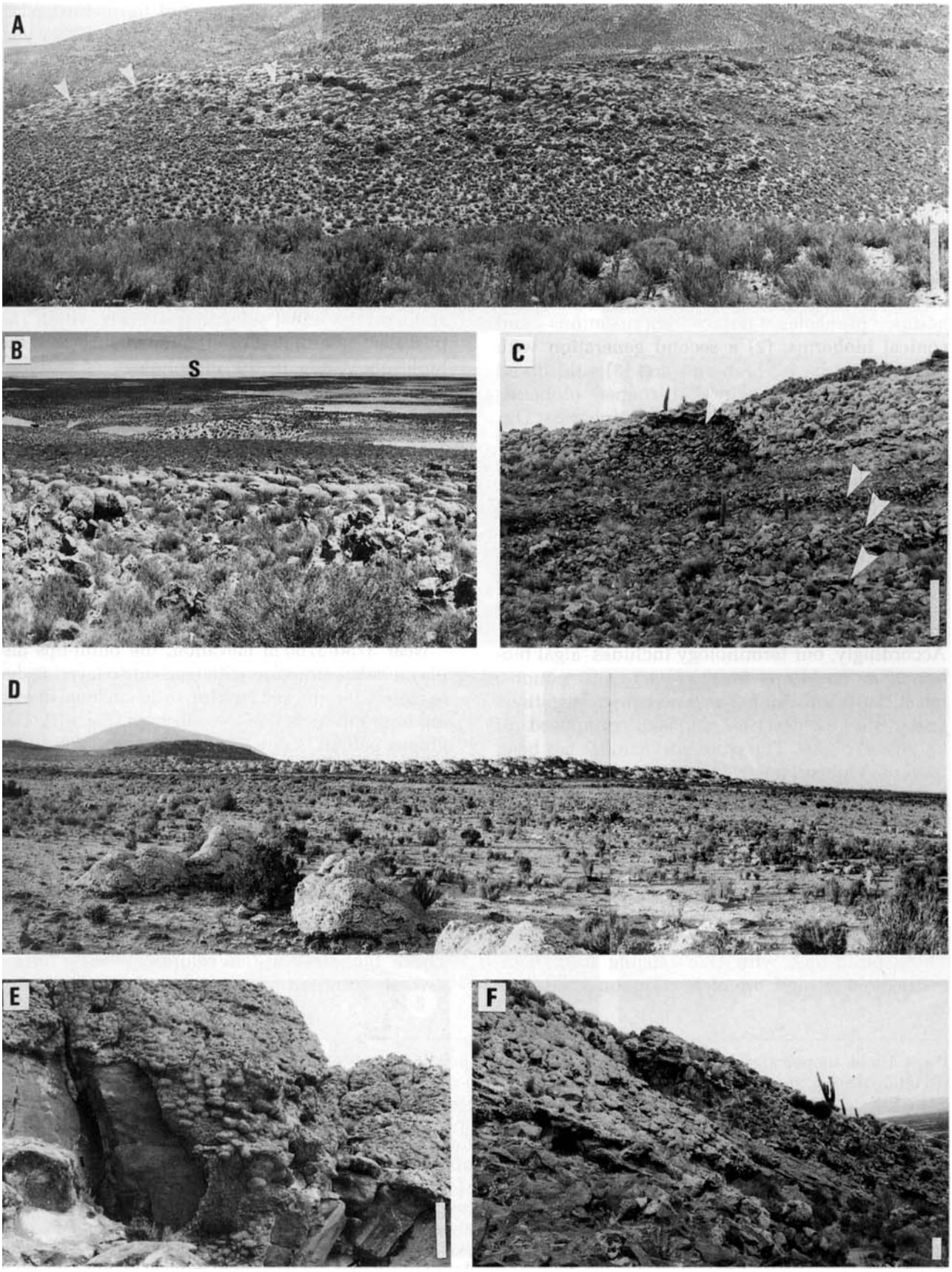
A
B
S
C
D
E
F

conditions, nature of the bedrock and erosional features (Fig. 2). The substrate is composed of either volcanic flows, volcaniclastic deposits, chaotic accumulations of volcanic boulders, the ragged surface of Palaeozoic schists or lacustrine sediments.

BIOHERM MORPHOLOGIES

Rondeau (1990) classified these carbonates as stromatolites belonging to three generations: (1) the oldest generation including massive bioherms, pinnacles, terrace encrustations and conical bioherms; (2) a second generation with flat and tart-shaped bioherms and (3) a third and younger generation with ball-shaped bioherms and encrustations upon blocks or bioherms. Our new field observations led us to adopt a different classification to avoid as much as possible the overlap between the generations and morphological types, and to account for the polygenic sequence of construction. Moreover, we show that these bioherms are not stromatolites in the sense of organosedimentary structures involving the activity of cyanophytes. The main builders are different communities of algae and other plants. Accordingly, our terminology includes 'algal bioherms' or 'build-ups' for the larger constructions, 'algal crusts' for thinner and planar encrustations and 'tufa' to describe deposits composed of encrusted plants. The word stromatolite has been used only for carbonate deposits displaying both a laminated pattern and organic remains which indicate they were built mainly by cyanobacterial communities. The term microbial encrustation is used when these features are less apparent.

Dome-shaped bioherms

These build-ups, with size ranging from decimetres to 4 m high, are most common at all sites between 3710 and 3750 m and formed extended carbonate lenses on the terraces at 3720 and 3740 m (Figs 2, 3 and 4A,B). They are predominantly characterized by either gently or steeply convex domal shapes, but include cylindrical, hemispheroid, club-shaped and tabular morphologies (Fig. 4A–C). They may coalesce upon the outer part of the terraces to form reef-like bodies near the break of slope (Fig. 4C). The domes often correspond to a carbonate algal crust several centimetres to 80 cm thick coating substrate protuberances that control both the size and the shape of the bioherms, e.g. volcanic boulders, spurs on the schist substrate, etc. (Fig. 4B,E). The pustular, mamillated or crenulated surface of the build-up is due to the morphology of the algal colonies mostly composed of branching tufts or bushes ranging from several centimetres to about 50 cm in length (Fig. 4D,F). The algal colonies may be directly fixed on either the substrate or an older algal crust in the composite build-ups (Fig. 4F). Although the outer surface of build-ups has usually been removed by erosion, many display a thin laminated stromatolitic crust that envelops the heads of the algal colonies (Fig. 4G). This outermost stromatolitic crust is generally better preserved on the steep palaeoslopes.

Near 3750/3760 m elevation, the build-ups display a radial structure with concentric layering due to closely interlocked fans (up to 50 cm long) diverging from the surface of the substrate (Fig. 4H). This fibrous pattern is due to the presence of sheaves of algal tubes probably similar to those that constitute the branching colonies. These bioherms have been intensely eroded, suggesting the elevation of the maximum lake highstand could have been only slightly higher than their present elevation.

Giant composite bioherms

These bioherms are developed over a terrace several hundred metres to 1 km wide that

Fig. 4. Dome-shaped algal bioherms. (A) Typical dome-shaped bioherms. 3740 m terrace at Huacuyo. Scale bar=1 m. (B) Internal structure of a domal build up composed of a 50-cm-thick algal crust (a) enveloping volcanic boulders (v). Scale bar=50 cm. (C) Aggregated build-ups displaying a reef-like pattern toward the break of slope of the 3740-m terrace. A thin laminated crust (arrows) covers the build-ups. Scale bar=1 m. (D) Outer surface of a bioherm with a bulbous aspect produced by the external morphologies of large algal sheaves. Huacuyo. Scale bar=5 cm. (E). Build-ups composed of a thin carbonate crust (arrows) coating large volcanic boulders. Churacari. Scale bar=20 cm. (F) Composite crust formed of two envelopes; the inner one (a) is composed of dense branching tufa and the outer one (b) shows larger bushy tufa. Small columnar stromatolites. Huacuyo. Scale bar=20 cm. (G) Bushy algal tufa (a) grading upward into aggregates of small columnar stromatolites (b) and ending by a dark stromatolitic laminated crust (s) which forms the external surface of the inner envelope. Palaeoslope near 3730 m of elevation. Huacuyo. Scale bar=2 cm. (H) Typical structure of the highest algal build-ups which are composed of large fibrous fans up to several decimetres long exhibiting discrete concentric bands. Huacuyo. Scale bar=1 cm.

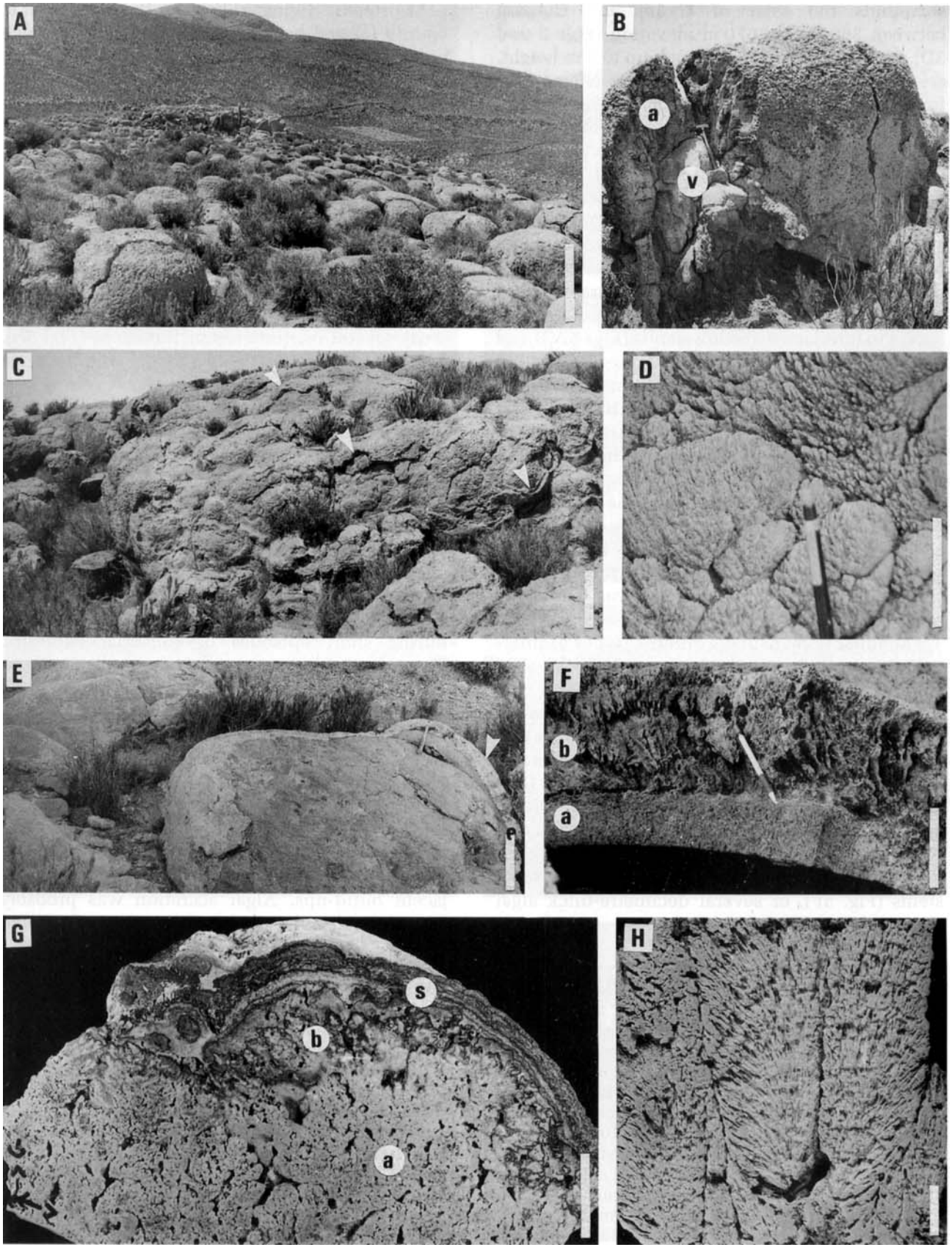

surrounds the salar of Uyuni and Coipasa between 3665 and 3670 m elevation (Figs 2 and 3D). The build-ups, which reach up to 5 m height, are mostly developed on the highs where they form small carbonate platform or reef-like aggregates (Figs 3D and 5A). Although domal shapes are still common, these build-ups generally exhibit complex morphologies that resemble carbonate pinnacles described at Searles and Pyramid lakes (Scholl, 1960; Benson, 1994, 1995).

The organization of the build-ups commonly shows two or three distinct parts formed during different lacustrine stages and separated from each other by major discontinuities which correspond to interlacustrine lowstands (Figs 5A,B and 6). At Estancia Sivingani the build-ups usually comprise an inner domal to columnar core that controls the general morphology of the build-ups and an isopachous or disymmetric envelope 5–90 cm thick that entirely wraps the inner core down to the foot of the bioherm (Figs 5B and 6). This envelope is divided into an inner layer up to 80 cm thick and an outer one whose thickness is generally less than 10 cm (Figs 5B and 6). Dissolutional features on the surface of the build-ups show that part of the outer layer has been removed.

The inner core displays different types of internal structure due to both the shapes of algal colonies and the relative amount of algae and internal sediment that fills up the space between the colonies. This can be dense structureless tufa made of a network of closely interlocked stems (Fig. 5C), balls of radiating algal colonies (Fig. 5D), isolated algal bushes embedded within sedimentary deposits or thinner layered algal tufa that moulds the surface of the colonies (Fig. 5E), decimetre-thick tubular tufa layers made of erect stems (Fig. 5F), or several decimetre-thick algal sheaves (Fig. 5G).

At Estancia Sivingani (Fig. 1), the inner layer is mainly formed by centimetre- to decimetre-thick branching tufa, interlayered with discontinuous sedimentary deposits similar to those of the inner core (Fig. 6B). Discrete discontinuities indicate fluctuations in the processes of bioherm accretion due to minor oscillations of the lake level. The branching tufa layers are made of algal tufts which grew perpendicular to the surface of the inner core so that they could develop horizontally along the walls (Fig. 6B). A significant sedimentary change occurs in the outer part of the inner layer which is composed of small columnar stromatolites, locally overlain by an outer planar laminated crust several centimetres in thickness (Fig. 5H). Secondary domes up to 50 cm high, which are due to the growth of larger algal bushes passing outward to columnar or planar stromatolites, developed on the top and walls of the main build-ups during this period of deposition (Figs 5B and 6A).

The outer layer (5–10 cm in thickness) starts with a 1-cm-thick planar stromatolitic crust which grades outward into a succession of discontinuous centimetre-thick structureless tufa layers irregularly separated from each other by micritized dissolutional surfaces (Fig. 5I). This structure indicates interruptions of algal growth during short episodes of subaerial exposure. These unstable environmental conditions contrast with the apparent stability that occurred during formation of the inner core.

Internal sediments include gastropods, micritic peloids, algal fragments, detrital grains and smaller algal colonies forming centimetre-high patches or thin bioconstructed layers. Some sedimentary layers protrude from the surface of the build-ups, indicating that, during biohermal accretion, they were forming sedimentary bridges connecting adjacent build-ups. Algal accretion was probably initiated on highs of the sedimentary floor and

Fig. 5. Large composite bioherms. (A) General distribution of the bioherms which may be aggregated to form a carbonate platform on the terrace (black arrows) while individual isolated build-ups occur on slopes and in lows (white arrows). Estancia Sivingani. The approximate height of the build-up in the upper left corner is 4 m. (B) Detail of the composite bioherms showing the massive inner core (i) and the envelope (e). Estancia Sivingani. Scale bar=2 m. (C–G) Internal structure of the inner core. (C) Dense tufa composed of closely interlocked algal colonies. Estancia Sivingani. Scale bar=2 cm. (D) Large radiating balls. Estancia Sivingani. Scale bar=5 cm. (E) Algal bushes embedded within carbonate sediments and thin layers of algal colonies. Estancia Sivingani. Scale bar=2 cm. (F) Tubular tufa interlayered with massive tufa. Estancia Chic. Scale bar=5 cm. (G) Large vertically standing branched algal colonies. Tauca. Scale bar=5 cm. (H) Detail of the outermost border of the inner envelope showing the progressive encrustation of the branched colonies (a) by small columnar stromatolites (b) and the final development of an external laminated stromatolitic crust (c). Estancia Sivingani. Scale bar=2 cm. (I) Detail of the outer envelope that encrusts the vertical wall of a bioherm. The basal laminated stromatolitic crust (a) which encrusts the wall of the inner envelope is covered by weathered tufa deposit including small tufts of fibrous tufa (b) and structureless tufa (c) showing several dissolutional surfaces (arrows). At outcrop, the crust has been intensely weathered during Holocene exposure. Estancia Sivingani. Scale bar=2 cm.

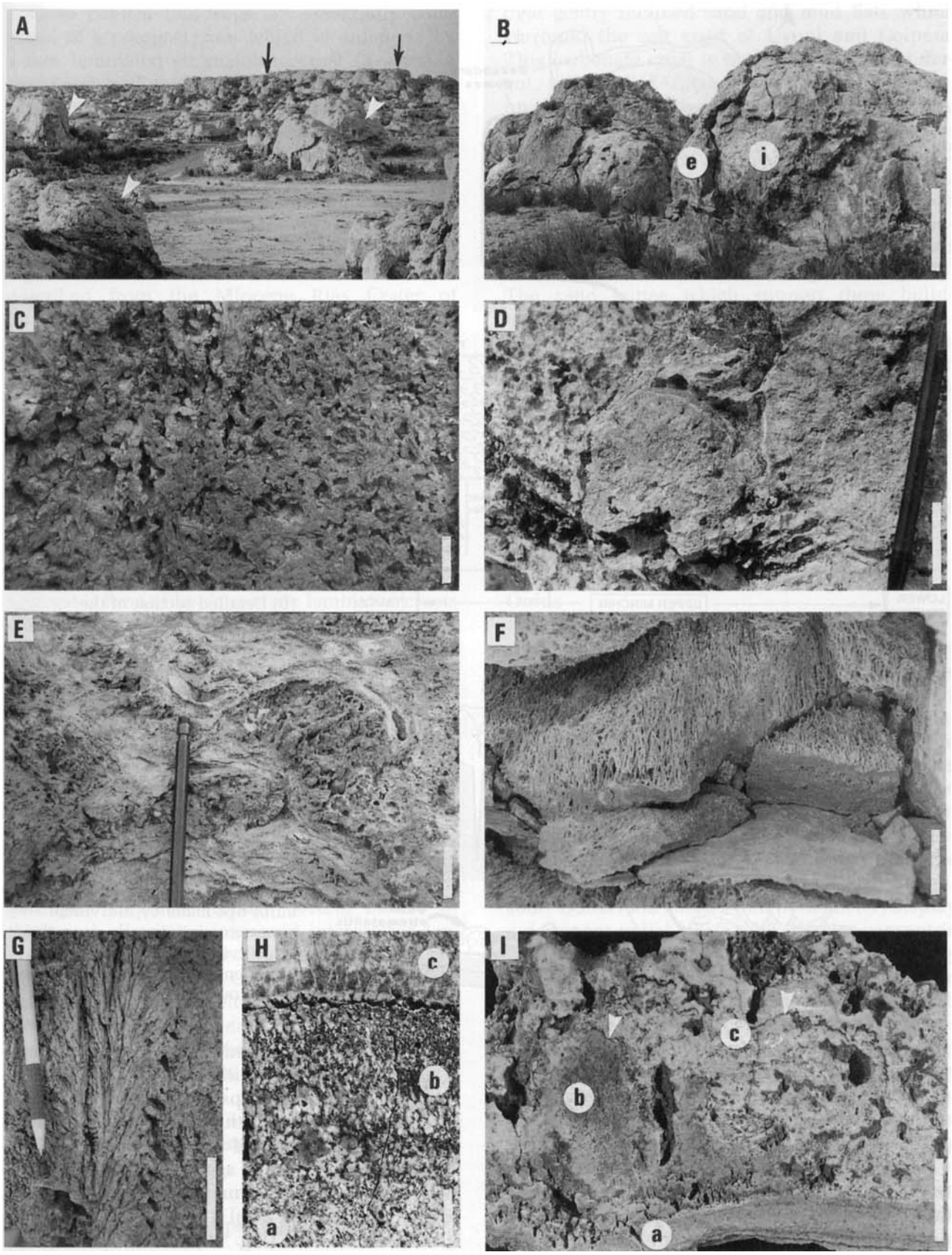
A
B
e
i
C
D
E
F
G
H
c
b
a
I
c
b
a

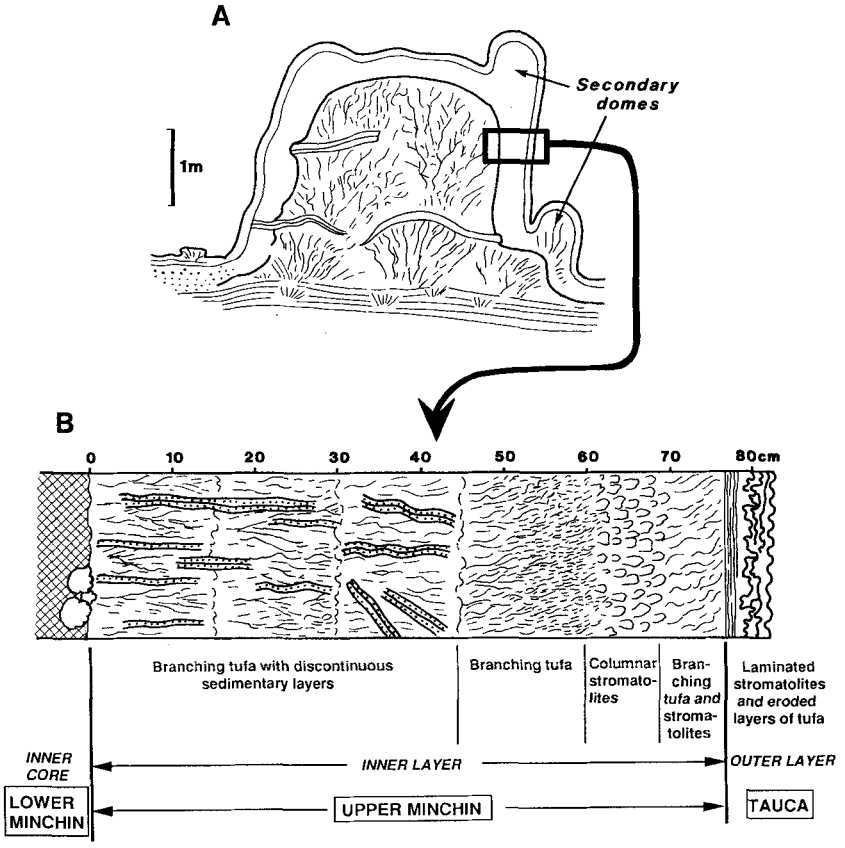

Fig. 6. Schematic organization of the giant composite bioherms. (A) Composite dome-shaped bioherm with an inner core mainly composed of branching tufa. The surface of the bioherm exhibits secondary smaller domes due to preferential development of large algal bushes in the inner layer. (B) Detailed section of the envelope.

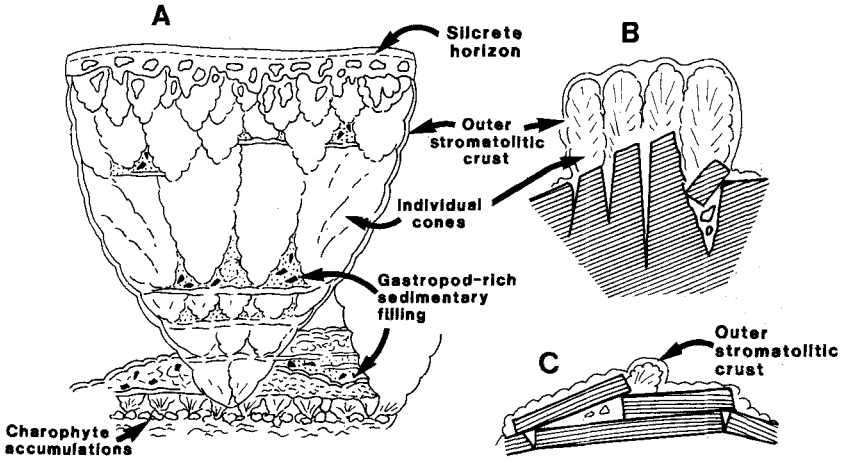

Fig. 7. (A) Schematic structure of the giant inverted cones from the Oruro area and its relations with the underlying sediment. Internal structure showing the relations between the individual cones. (B–C) Toward the land margin, the giant inverted cones are progressively replaced by smaller build-ups made by individual cones growing directly upon the schist basement (B) and then by direct encrustation of the basement by the outer laminated crust (C).

accreted synchronously with the deposition of lacustrine sediments (diatomites and claystones) in the interdomal lows.

Giant inverted conical bioherms

In the Oruro area (Fig. 1), a different type of algal build-up, characterized by giant inverted cones up to 4 m high and 4 m in diameter, is observed on the terrace at 3700 m (Fig. 7A). When these carbonate build-ups formed, this area was a distinct sub-basin separated from the main Coipasa–Uyuni basin by a sill located near 3715 m elevation. The build-ups grew mainly on lacustrine sediments. As with other types of build-up, the size and density of build-ups increase lakeward to form reef-like aggregates (Fig. 2). Landward, they grade into smaller bioherms composed of decimetre-high algal tufts directly fixed on Palaeozoic schists (Fig. 7B), while the substrate has been locally plastered by a centimetre-thick laminated crust (Fig. 7C).

These conical build-ups are essentially composed of a compact core which is onlapped by a thin laminated stromatolitic crust (3–4 cm in thickness), without evidence of an inner envelope as seen on the giant composite bioherms (Fig. 7A). The upper part of the cones may be intensely weathered, grading upward into a decimetre-thick layer of silcrete which has been eroded and accumulated as breccia between the bioherms (Figs 7A and 8A).

The external morphology, size and internal organization of the core is reminiscent of those described from the Miocene Ries Crater of Germany (Riding, 1979). The large inverted cones start with a narrow base, decimetre or less in diameter, and rapidly widen upward to 4 m in diameter (Figs 7A and 8A,B). Due to their lateral accretion, the adjacent domes coalesce at the top.

The surface of the bioherms displays a mamillary, bulbous or pustular appearance that frequently reflects the shape of elementary algal cones (Figs 7A,B and 8A–D). These decimetre-sized individual cones are composed of algal sheaves with radial structure, as well as rounded aggregates formed by concentric laminated crusts around plant stems or gastropod shells (Fig. 8E,F). Large amounts of sediment composed of volcaniclastic grains, peloids and gastropods fill internal voids and intercolumnar spaces. The elementary cones are enveloped by a decimetre-thick laminated crust similar to that which surrounds the bioherms (Figs 7A,C and 8E). Internal laminated encrustations are better developed in these deposits than in the other types of build-ups.

The algal build-ups accreted synchronously with the deposition of sediments comprising fine-grained terrigenous deposits, claystones, gastropod coquinas (locally several metres in thickness), diatomite oozes and intercalated layers or patches composed of Chara stems and small algal sheaves (Fig. 7A). Unlike most of the other build-ups that encrust blocks or basement irregularities, the conical bioherms grew on these lacustrine sediments. However, they did not nucleate on soft sediments, but on decimetre-thick carbonate layers composed of accumulations of Chara stems and algal sheaves with radial structure (Figs 7A and 8B,F,G), associated with large encrusted plant stems (Fig. 8H).

Miscellaneous build-ups of the 'low-terrace'

The 'low-terrace' is a 2–10-cm-thick peloidal, desiccation-cracked carbonate crust, developed over gently inclined sand and mud flats which surround the salt crust of Uyuni and Coipasa. This carbonate crust is locally covered by different varieties of tufa and stromatolitic build-ups. They comprise: (1) mushroom-like tufa several centimetres high formed by upward-diverging algal sheaves (Fig. 9A); (2) flat discoid build-ups 10 cm to 1 m in diameter and up to several decimetres in thickness (Fig. 9B) which consist of an inner core formed by local thickening of the basal crust on top of small sand buttes with a crown of branching tufa (Fig. 9C). The sand buttes which support these build-ups may have formed from trapping of wind-driven particles by erect grass tufts during an intra-Tauca subaerial exposure of the mudflat; (3) cylindrical laminated tufa up to 10 cm thick encrusting large wood fragments (Fig. 9D); (4) large pisolitic tufa decimetres in diameter with an inner core built by the centrifugal growth of algal colonies enveloped by a centimetre-thick stromatolitic layer attached to the 'low-terrace' carbonate crust (Fig. 9E).

Ooids

Accumulations of ooids or coated grains occur at two sites near Tauca (Fig. 1). At the first site, the coated grains are disseminated in the upper part of fan terrigenous deposits composed of a fining-upward sequence of gravels and sands. At the second site, the deposit is not seen *in situ*, but as large stones coming from the bioherms of the 3660–3680 m terrace. The ooid-rich deposits form decimetre-sized aggregates of irregular shape, encrusted by stromatolites. At the two sites, the ooids formed during a pre-Tauca lacustrine episode. Ooids (300 μm to 2 mm in diameter) display a dominant radial fabric with discrete concentric cortical layers. The cortex is frequently crossed by undulating fibres or filaments less than 15 μm in diameter which may be isolated or grouped in fans. The ooids may contain a detrital nucleus while detrital grains are commonly included within the cortex. The ooid aggregates commonly display a close-packed fabric with sutured contacts between grains that probably result from intergrowth processes rather than compaction. These ooid deposits could represent either accumulations of ooids trapped in the spaces between algal constructions or *in-situ* growth within large voids of the cavernous carbonate build-ups, as reported in stromatolites from the Magadi Lake (Casanova, 1994).

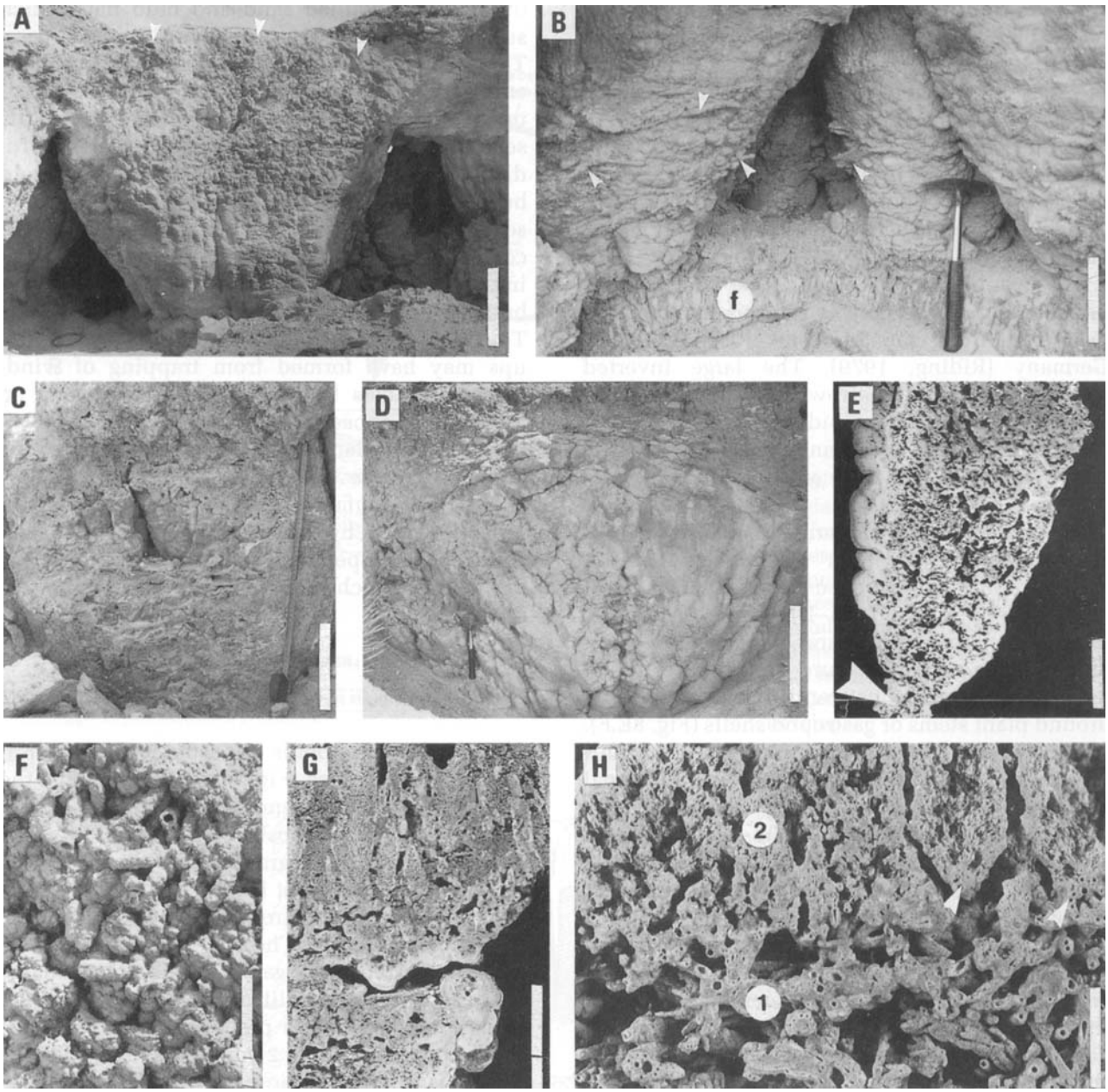

Fig. 8. Giant inverted cones from the Oruro area. (A) Massive inverted cone. The build-ups are separated from each other by large voids initially filled with lacustrine sediments. The build-ups widen upward to coalesce in their uppermost part. Their upper part is covered by a layer of silcrete (arrows) that may be reworked as breccia in the interdomal depressions. Scale bar=1 m. (B) Base of the cones showing the narrow foot, nucleated on a decimetre layer composed of vertically standing fans of fibrous tufa (f) resting on accumulations of *Chara* stems shown in (H). The surface of the build-ups display a bulbous to pustular morphology as well as remnants of carbonate layers which were intercalated in the fill between the cones (white arrows). Hammer is 37 cm high. (C) Small composite cone showing the internal structure composed of numerous smaller individual cones. Scale bar=20 cm. (D) Composite cone composed of radially orientated individual cones. Scale bar=50 cm. (E) Detail of an individual cone showing the outer laminated stromatolitic crust that covers the inner core. The core is made of aggregates of algal colonies and internal sediments. The growth of this cone seems to have been initiated around a plant stem (arrow). Scale bar=50 cm. (F) Tubular tufa observed in the basal part of a build-up. Scale bar=1 cm. (G) Structure of the basal part of a cone which is composed of charophytes enveloped by laminated crusts in the lower half of the sample and vertically standing fans of fibrous tufa in the upper half. Scale bar=1 cm. (H) Detail of the basal carbonate layer upon which the cones nucleated. The accumulation of *Chara* stems (1) on the sediment surface are used as substrate for the growth of the colonies of other green algae which form here small inverted cones (2) with a fibrous structure. Some of the fibrous fans start growth directly on a *Chara* stem (arrows). Scale bar=1 cm.

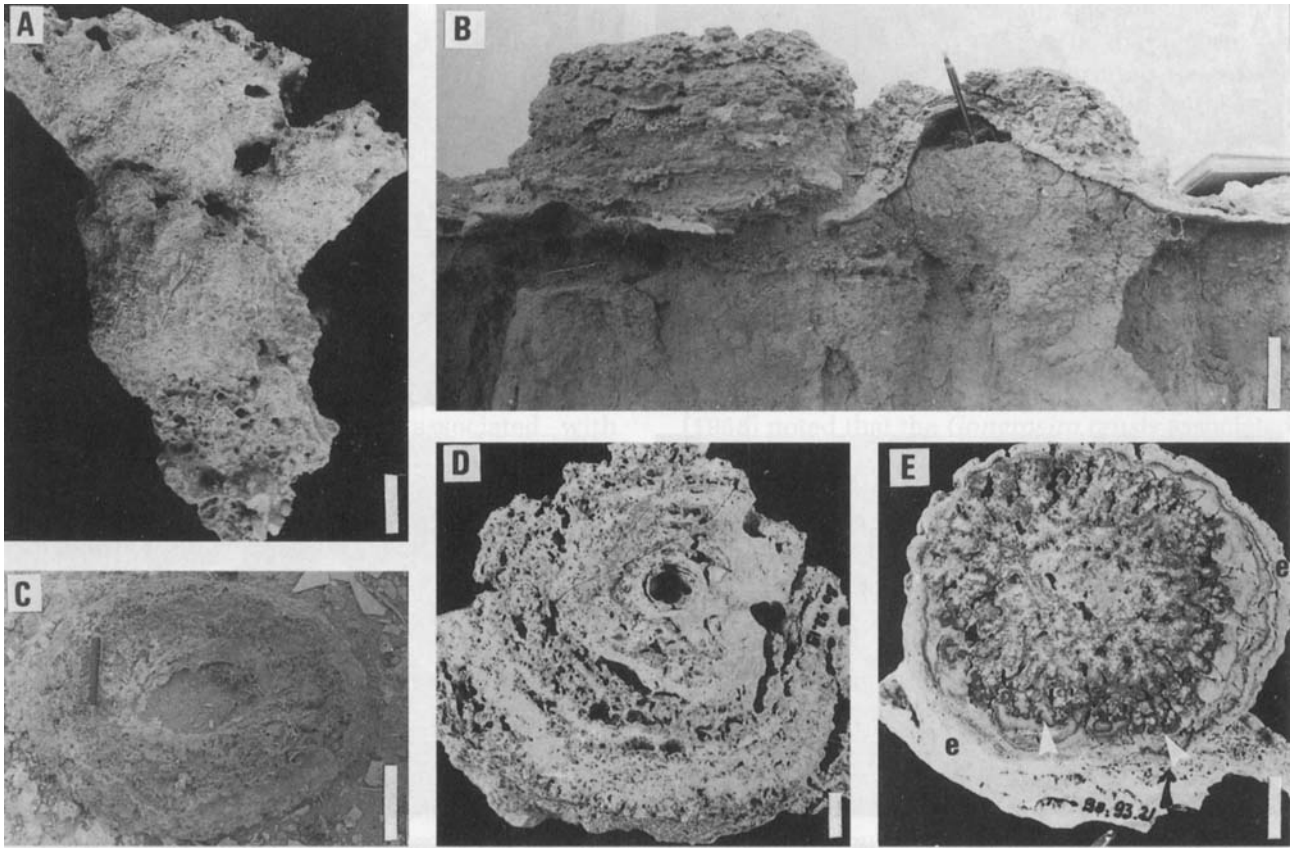

Fig. 9. Small algal build-ups of the low terrace (3653–3655 m elevation). (A) Mushroom-like constructions. Estancia Sivingani. Scale bar=1 cm. (B) Discoid build-ups. The section of the right build-up shows that it is composed of a crown developed around a thickening of the low-terrace crust on top of sandy bumps on the lacustrine sediment. Tauca. Scale bar=10 cm. (C) Plan view of the discoid build ups showing its ring shape. Scale bar=10 cm. (D) Large concentrically laminated tufa encrusting wood fragments at the surface of the low terrace. Estancia Sivingani. Scale bar=1 cm. (E) Large pisolitic tufa with radial structure. The radial aggregates of algae which form the centre of the pisoid grade outward into dark stromatolitic crusts displaying small branched to digitate stromatolite constructions (arrows). An outermost laminated crust (e) envelopes the pisoid and links it to the carbonate crust of the low terrace. Scale bar=1 cm.

COMPOSITION AND MICROSTRUCTURES

Bulk sample analyses of various types of bio-constructed carbonates show that the carbonate fraction is exclusively composed of low-Mg calcite (up to 4 mol% $MgCO_3$). Aragonite has only been detected in a peloidal lamina included within the thin laminar crust of the Tauca low-terrace. Other components consist mainly of small detrital grains, i.e. quartz, micas, feldspars, minerals of volcanic origin, and locally volcano-sedimentary or Palaeozoic clasts.

Calcite cements

There are three main groups of calcite cements. The first group includes various types of aggregates of clear radial sparry calcite, several hundred micrometres to several millimetres long: (1) closely interlocked or isolated aggregates of fascicular crystals which may diverge from a central zone usually occupied by a section of plant stems (Fig. 10A,B) – some resembling bundles of radiating calcite described in the pisoliths from the Laguna Pastos Grandes, in the Lipez area (Risacher & Eugster, 1979; Jones & Renaut, 1994); (2) fan-shaped hemispheroids that occur as isolated fans in the micritic laminated crusts or as aggregates which form either sparitic layers within the stromatolites or complex concentric crusts around stems, algal tufts or other components (Fig. 10C,D). These calcite cements enclose ghosts of filaments, 2–5 μm in diameter and up to 300 μm long, which may be irregularly disseminated within the spar or arranged as

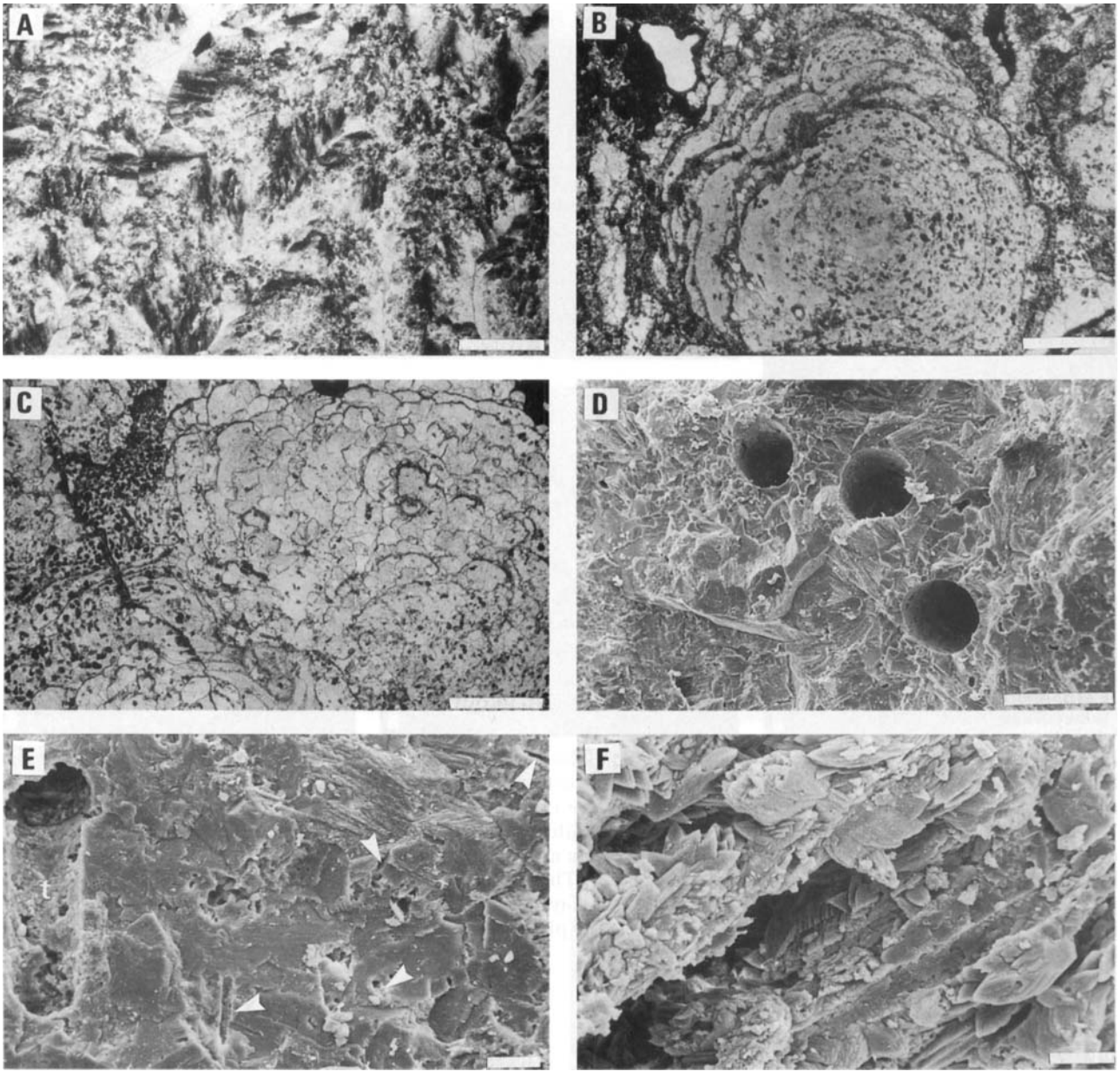

Fig. 10. Calcite cements. (A) Closely interlocked aggregates of sparry calcite fans. Photomicrograph, crossed nicols. Scale bar=1 mm. (B) Concentric cements which grade outward into alternating micrite laminae and sparry mamelons (cellular fabric). The calcite cement includes sections of empty tubes as well as concentrically arranged micritic grains. Photomicrograph, plane light. Scale bar=100 μm. (C) Concentric aggregates of sparitic hemispheroids containing both sections of empty tubes and small micritic grains. Photomicrograph, plane light. Scale bar=1 mm. (D) Radial sparry calcite cements around empty tubes. SEM. Scale bar=100 μm. (E) Radial sparry cements including two types of plant remains: large empty tubes (t) and small filaments about 2·5 mm in diameter (white arrows). SEM. Scale bar=20 μm. (F) Small elongated crystals sheathing filaments in the fibrous tufa. SEM. Scale bar=20 μm.

diverging sheaves (Fig. 10E). The second group, mainly fibrous-like tufa, is composed of aggregates of euhedral to subhedral elongated crystals (5–50 μm) that sheath or replace the algal filaments and fill the spaces between them (Fig. 10F). The third group are large isopachous sparry calcite fringes developed around internal cavities.

Algal communities and microfacies

The major part of the bioherms consists of tufas deposits with structure (branching tufa, tubular tufa, large bushes or balls) that suggests they were constructed by the *in-situ* growth of subaquatic vegetation. The size and shapes suggest the major

builders were not cyanobacterial communities but various kinds of filamentous microflora and macrophytes.

Main microflora communities

Although the plant communities responsible for the building of these bioherms were undoubtedly more complex, two dominant types are recognized by the macroscopic shape of the colonies and their microstructures.

1 The massive, tubular, spheroidal and some branching tufas commonly display two different vegetal ghosts intimately associated with encrustations of radial sparry calcite: (i) tubes 50–200 μm in diameter, empty or filled with either monocrystalline calcite or micrite. These usually constitute the centre of the radial sparry aggregates or are disseminated within them (Figs 10B,D and 11A–D). These structures are attributed to plants forming dense networks or bushy tufts. (ii) Small circular to ovoid micritic bodies, 20–150 μm in diameter (mean 50–90 μm), concentrically distributed in the sparry aggregates around a central stem (Figs 10C and 11A). These look like peloids, but their concentric distribution around larger plant ghosts suggests they are remnants of epiphytic plants attached to the surface of larger stems. Large accumulations of these micritic components form a densely clotted microfabric as seen in the mushroom-like build-ups of the low-terrace (Fig. 11C).

2 The bushy, radial and occasionally branching tufas generally have a filamentous structure (Figs 4G,H, 8G,H and 11E). These filaments, averaging 40–60 μm in external diameter, are composed of a calcite sheath coating an internal tube 8–20 μm in diameter (mean 10 μm) (Fig. 11F,G). Sometimes, the calcite filling of the tubes exhibits an internal partition which suggests cell boundaries (Fig. 11G). Filaments of identical internal size may also form small cushions or balls (Fig. 11H).

Taxonomic identification of these plants is problematic. The shapes, internal structures and size of the two main frame building plants are not similar to microbial remains. The similarity between the large inverted cones of the Oruro sub-basin with those from the Miocene Ries Crater in Germany, which are built by an epilithic green algae *(Cladophorites)* (Riding, 1979), suggests the Altiplano bioherms are built by colonies of calcifying filamentous green algae. Three modern epilithic fresh-water chlorophytes (*Cladophora*, *Gongrosira* and *Oocardium*) are known to calcify and form balls and cushions up to 30 cm high (Smith, 1950; Golubic & Fisher, 1975; Pentecost, 1988, 1991). The diameter of the larger filaments (50–200 μm) forming the centre of the encrusted aggregates is similar to those of *Cladophorites* from the Ries Crater (90–180 μm), while those of the branched sheaves of filaments (20–50 μm) are similar to those of the modern *Cladophora* (10–50 μm) (Smith, 1950; Osborne *et al.*, 1982). The radiating sheaves of filaments which form some fibrous aggregates closely resemble cushions of *Cladophora* or *Gongrosira* described in diverse modern freshwater settings (Smith, 1950; Golubic & Fisher, 1975). Pentecost (1988) noted that the *Gongrosira* crusts associated with the cyanobacterial deposits in the ponds of Quatro Ciénegas (Mexico) could be confused with microbialites and that the 'encrusted colonies closely resemble those of cyanobacteria' so that the 'interpretation of fossil material would be difficult'.

Charophytes are rarely observed within the build-up frame, except in some tubular or branching tufa. The larger accumulations of *Chara* stems are present within and on top of lacustrine sedimentary sequences where they form hard bottom layers. Other communities of unidentified higher plants contributed to the building frame, as for example those forming the tubular tufas. Some stems of higher plants supported epiphytic growth of filamentous algae, as observed in the lower part of the inverted cones (Fig. 8E).

Diatom associations

Ghosts of diatom frustules are occasionally present in the spar fringe, although denser accumulations occur in places (Fig. 11H). A preliminary survey indicates that the assemblages contain species common in the lacustrine sediments of the Altiplano basin (*Cyclotella*, *Rhopalodia*, *Epithemia*) and those characteristic of saline conditions (S. Servant-Vildary, pers. comm.).

Microbial communities

The most striking feature of these carbonate build-ups is the limited development of stromatolites. Although Rondeau (1990) identified the presence of *Rivularia* and *Phormidium encrustatum*, these cyanobacteria did not contribute significantly to construction of the bioherm frame. Instead they formed thin (<5 cm thick) laminated envelopes coating the build-ups and encrustations around various supports, i.e. colonies of green algae, macrophytes or shells.

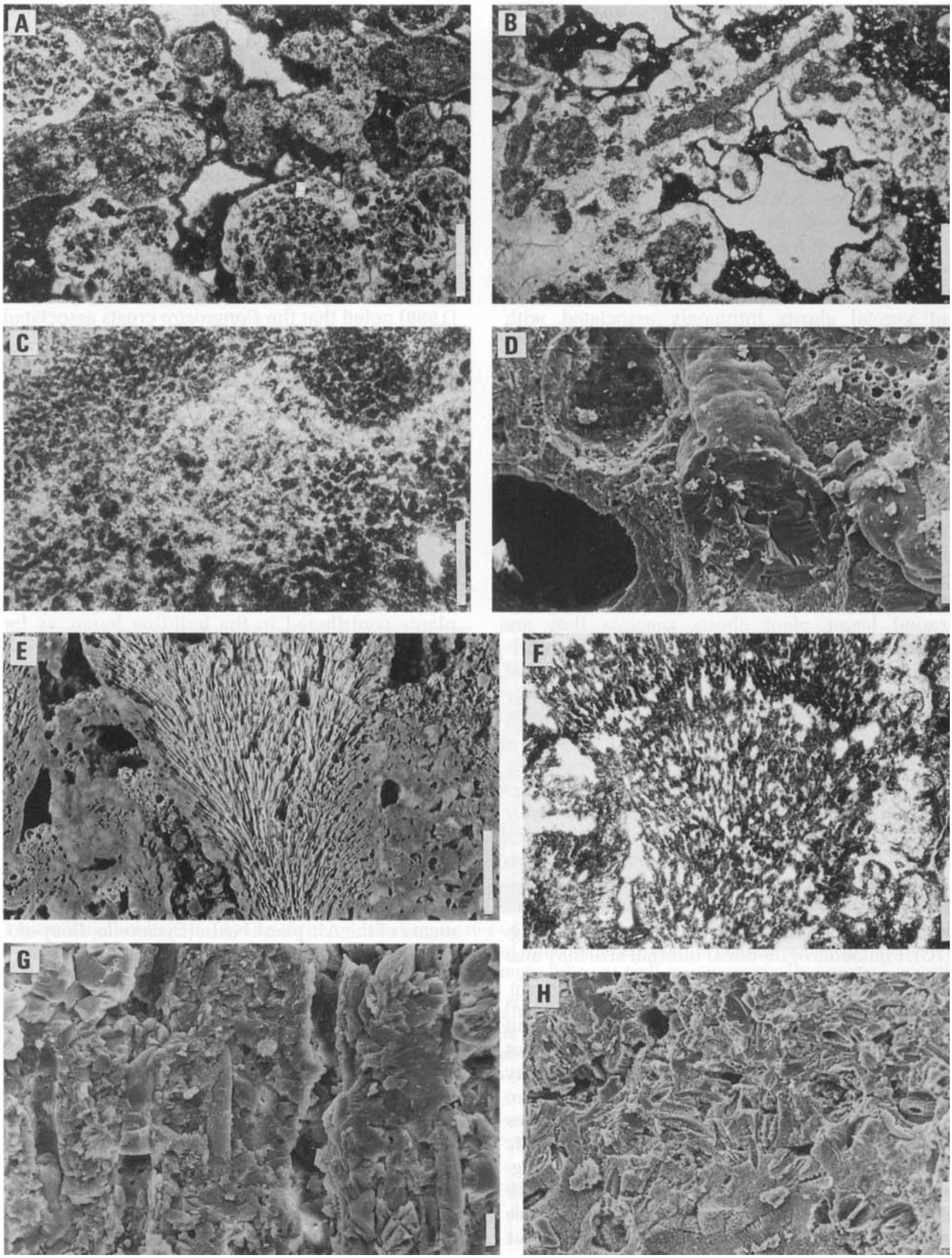
A
B
C
D
E
F
G
H

There are three types of microbially induced deposits: (i) planar to gently undulating laminated crusts that coat the surface of build-ups and algal cones (Figs 4G, 5H,I, 6C, 8E and 12A,B); (ii) small columnar bodies (Figs 6E, 8H and 12C,D); (iii) concentric encrustations around algal stems or skeletal components in the build-up frame, especially in the giant inverted cones (12E). Similar columnar and concentric crusts are also known in the pisoliths from the Laguna Pastos Grandes (Jones & Renaut, 1994). Although less common, there are also small micritic microdomal bodies attached to the walls of internal cavities. The microstructure of the laminated crusts is determined by the relative proportion of either micritic or clear sparitic laminae (Fig. 12A–D); the sparitic laminae may be formed by more or less isopachous layers, hemispheroids or mamelons of radial sparry calcite, whereas scattered hemispheroids isolated within the micritic laminae produce a cellular fabric (Fig. 12A,D). Sparry encrustations which form concentric envelopes around various plant remains grade upward into columnar to branched stomatolites (Fig. 12C,D) so that all these features may be considered more or less directly linked with processes of stromatolitic accretion. These sparry cements enclose filaments 2–5 μm in diameter which may be scattered or assembled to form erect tufts or sheaves (Fig. 12F). This development of polycyclic sparry and micritic laminae, common in many phytoherm deposits, is interpreted as resulting from seasonal processes of biologically induced micrite and precipitation of a spar fringe which may be either biologically mediated or due to an inorganic crystallization incorporating the cyanophyte trichoms (Casanova, 1986; Pedley, 1992).

The microbially related encrustations around algal colonies may have indurated the constructions, thereby helping to preserve their morphologies. Except for the epiphytic microbial communities attached on both living or decayed higher plants, stromatolites formed at the end and the beginning of biohermal accretion. This suggests that the microbial activity replaced chlorophyte and other higher plant development when environmental conditions became more unstable during rising or falling lake level.

DISCUSSION

One of the most striking features of the Altiplano carbonate bioherms is their polygenic construction due to repeated growth of algal communities during successive lacustrine highstands. A similar composite organization of build-ups has been described in some pinnacles developed on the palaeoslopes of Lahontan Lake, in North America (Benson, 1994, 1995). Between 3660 and 3680 m elevation (Estancia Sivingani) the build-ups display up to three different stages of growth; two main stages are still present up to 3730 m while a single crust occurs up to 3750–3760 m which is the highest elevation at which algal carbonate deposits have been observed. The U/Th and radiocarbon ages (15 ka) obtained on this crust indicate the higher lake level occurred during the Tauca episode (Causse *et al.*, 1995; Servant *et al.*, 1995). At this time, the lake occupied an area of at least 80 000 km^2 (Servant *et al.*, 1995) with a water depth near 100–110 m. Indeed, the lake level could have risen somewhat higher, as the fragmented appearance of these crusts indicates this upper limit is eroded.

The three parts which form the giant composite bioherms between 3660 and 3680 m (Fig. 6) comprise an initial dome-shaped build-up formed during an old lacustrine stage and two superimposed layers whose U/Th ages are, respectively, *c.* 40 ka (upper Minchin episode) and 16 ka (Tauca episode) (Causse *et al.*, 1995). This last date, obtained on the stromatolitic crust located at

Fig. 11. Algal remnants. (A) Microfabric of the radiating balls which form the inner core of the giant composite bioherms: circular aggregates of sparry calcite including micritic bodies which appear concentrically arranged around the centre of the aggregates. Photomicrograph, plane light. Scale bar=1 mm. (B) Microfabric of the branching tufa displaying sections of micritic tubes with an empty central zone, encrusted by aggregates of radial sparry calcite. Photomicrograph, plane light. Scale bar=1 mm. (C) Microfabric of the mushroom-like build-ups: clotted structure due to dense aggregates of micritic bodies with a circular to elongated section. Scale bar=500 μm. (D) SEM view of the large filaments which form most of the branched tufa, filled here by monocrystalline calcite. Scale bar=50 μm. (E) Fan of fibrous tufa included within deposits formed of encrusted larger tubes including *Chara* stems and gastropod-rich sediment. Scale bar=1 cm. (F) Typical microfabric of the fibrous tufa formed of filament bushes displaying a radial pattern with some concentric growth bands. Photomicrograph, plane light. Scale bar=10 μm. (G) SEM view of fibrous tufa showing the filaments included within a mosaic of calcite. Scale bar=10 μm. (H) Abundant moulds of diatoms in the sparry calcite. SEM. Scale bar=50 μm.

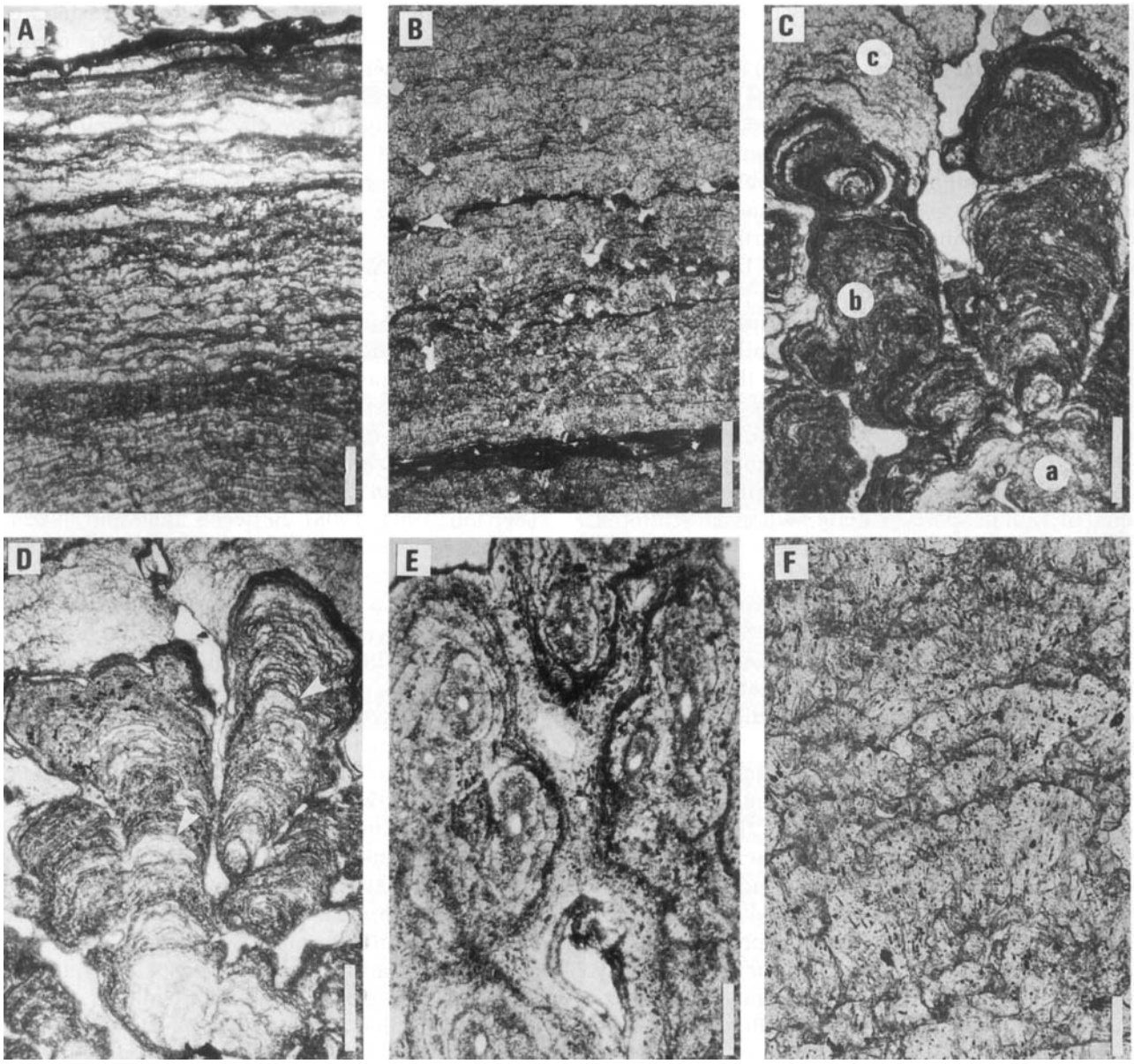

Fig. 12. Microbially induced microfabrics. (A) Laminated crust made of variable proportions of clear sparry layers and micritic laminae. The sparry layers may be composed of hemispheroids or mamelons that produce a cellular fabric. Photomicrograph, plane light. Scale bar=500 μm. (B) Laminated crust mainly composed of clear sparitic laminae. Photomicrograph, plane light. Scale bar=1 mm. (C) Branched columnar stromatolitic fabric. The stromatolitic accretion starts around aggregates of sparry cements (a), then grades transitionally into a finely laminated crust dominantly made of micritic laminae in the lower part (b) and clear sparry layers in the upper part (c). Photomicrograph, plane light. Scale bar=1 mm. (D) Same features showing the development of a cellular fabric (arrows). Photomicrograph, plane light. Scale bar=1 mm. (E) Concentric encrustations of algal tubes composed of alternating clear sparry layers and micritic laminae similar to that which composes the stromatolitic crusts. Photomicrograph, plane light. Scale bar=500 μm. (F) Close-up of the sparry layers or mamelons showing sheaves of filaments included in the calcite crystal aggregates of sparry calcite. Photomicrograph, plane light. Scale bar=100 μm.

the base of the outer layer, shows this layer formed during the Tauca lake level rise. The low terrace build-ups formed later during the small lake level rise that occurred at the end of the Last Glacial stage (Coipasa event, around 11 ^{14}C ka BP) (Servant *et al.*, 1995; Sylvestre *et al.*, in press).

During the Minchin episodes, the water depth was shallower than during the Tauca highstand,

but accurate evaluation requires further dating of the carbonate deposits. The interlacustrine lowstands caused only moderate erosion and weathering of the carbonate build-ups at low elevation. During interlacustrine lowstands, the water level fall ended in the desiccation of the basin and the deposition of thick salt layers in the deeper depression of Uyuni where halite beds several metres thick are intercalated within claystones and siltstones. These important, although short-lived, periods of subaerial exposure which affected the marginal carbonate deposits during the hypersaline episodes did not induce the development of well-developed erosional disconformities.

Except for the giant build-ups in the Miocene of the Ries Crater of Germany (Riding, 1979), calcified green algae were not previously known to generate large carbonate constructions. Calcified green algae are known to form small build-ups in association with calcified cyanobacteria, which are the main builder (Golubic & Fisher, 1975; Wood, 1975; Osborne *et al.,* 1982; Pentecost, 1991; Winsborough *et al.,* 1994). Except for local occurrences of diatoms in the calcite cements, and although a high diatom productivity occurred lakeward, we do not have evidence that diatoms were important to build-up growth.

The conditions responsible for both this unusual development of green algae and their potential to generate extensive carbonate accumulations is not yet clearly understood. The carbonate build-ups are observed in such an extended distribution and diversity of settings that it is evident their growth has been controlled by the physicochemical conditions of the lake, not by thermal water springs as reported in many other settings. Water depth was not a discriminating parameter for the development of either calcified green algae or cyanobacteria as they probably both developed in relatively shallow conditions during either rise or fall of lake level. In contrast, the lake level dynamics may have favoured the development of either green algae during stationary lacustrine stands or microbial communities during periods of unstable conditions. Hydrological closure may have influenced the growth dynamics and favoured a greater microbial development as in the Oruro sub-basin.

The calcium content of the lake waters was provided by weathering of the catchment strata, mainly volcanic rocks, but also some Upper Cretaceous/Tertiary carbonates and calcium sulphates. Salinity may have varied, during the formation of these carbonate deposits, from less than 5 g L^{-1} to values as high as 80 g L^{-1} with a dominantly sodic composition (Servant-Vildary, 1978; Rondeau, 1990; Risacher & Fritz, 1991; Risacher, 1992; Wirrmann & Mourguiart, 1995; Sylvestre *et al.,* in press). Carbonates did not precipitate spontaneously from the lake waters as they are not present in the sections of lacustrine sediments observed in various cores or outcrops where the deposits are exclusively composed of clays, silts and diatom oozes. The evaporitic succession that precipitated in the salar of Uyuni during interlacustrine lowstands is predominantly composed of halite with 1–10% calcium sulphate in the uppermost halite layer. This suggests that most of the dissolved calcium was trapped by the luxuriant algal development along the shores of the basin. Factors that favoured the precipitation of carbonates in relation to plant development are difficult to determine. However, it is clear that the uptake of CO_2 due to the metabolic activity of these plant communities was a major factor in influencing calcium carbonate precipitation.

SUMMARY

The Pleistocene lakes of the central Altiplano provide one of the most extensive developments of lacustrine algal bioherms presently known. The bioherms are characterized by repeated growth during at least three main lacustrine highstands and the builder communities were dominated by filamentous calcifying green algae associated with other plants. Although the morphologies are reminiscent of stromatolites, microbial communities did not contribute significantly to the construction of bioherm frames. The difficulties in differentiating some filamentous green algae from cyanobacteria could be the reason that these types of algal constructions are so rarely reported from old lacustrine deposits. The algal growth was locally so active that it led to the formation of small carbonate platforms and reef-like lenses. During interlacustrine episodes, the drop of the lake level provoked the periodic subaerial exposure of the bioherms, but the resultant erosional discontinuities which separate the successive phases of construction are locally so discrete that they could easily escape observation in older deposits. Each of these discrete discontinuities is coeval with the deposition of thick salt layers in the deepest part of the basin represented by the salar of Uyuni.

ACKNOWLEDGMENTS

This research was part of the objectives of programmes supported by the BQR-Museum. Field investigations have been funded by both this programme and by the Institut Français d'Etudes Andines through C. de Muizon, whereas the Mission Bolivie of the ORSTOM provided the field logistics. Special thanks are due to J. Launay and R. Soler for their help in the organization of the field trip, Ph. Mourguiart for his assistance on the field investigations, P. Ditchfield for improvement of an early draft of the manuscript and R. Riding for a short and fruitful discussion about the samples. B. Jones and J. Casanova provided a number of useful comments in reviewing the paper and J. E. Andrews greatly improved the final version of the manuscript. Thanks are due to P. Clement for his assistance in X-ray and SEM studies, M. Tamby for sample processing, M. Destarac for photography and A. Cambreleng for draughting.

REFERENCES

Benson, L. (1994) Carbonate deposition, Pyramid Lake Subbasin, Nevada: 1. Sequence of formation and elevational distribution of carbonate deposits (Tufas). *Palaeogeogr. Palaeoclimatol. Palaeoecol.*, **109,** 55–87.

Benson, L. (1995) Carbonate deposition, Pyramid Lake Subbasin, Nevada: 2. Lake levels and polar jet stream positions reconstructed from radiocarbon ages and elevation of carbonates (tufas) deposited in the Lahontan basin. *Palaeogeogr. Palaeoclimatol. Palaeoecol.*, **117,** 1–30.

Bertrand-Sarfati, J., Freytet, P. and Plaziat, J.C. (1966) Les calcaires concrétionnés de la limite Oligocène–Miocène des environs de Saint-Pourçain sur Sioule (Limagne d'Allier). Rôle des Algues dans leur édification, analogie avec les stromatolites et rapports avec la sédimentation. *Bull. Soc. Géol. Fr.*, **VIII**, 652–662.

Bertrand-Sarfati, J., Freytet, P. and Plaziat, J.C. (1994) Microstructures in Tertiary Nonmarine stromatolites (France). Comparison with Proterozoic. In: *Phanerozoic Stromatolites II* (Ed. by J. Bertrand-Sarfati and C. Monty), pp. 155–192. Kluwer Academic Publishers, Dordrecht.

Casanova, J. (1986) *Les stromatolithes continentaux: paléoécologie, paléohydrologie, paléoclimatologie. Application au Rift Gregory.* Thesis, University of Aix-Marseille II.

Casanova, J. (1992) Late Holocene hydrological history of lake Tanganyika, East Africa, from isotopic data of fossil assemblages. *Palaeogeogr. Palaeoclimatol. Palaeoecol.*, **91,** 35–48.

Casanova, J. (1994) Stromatolites from the East African Rift: a synopsis. In: *Phanerozoic Stromatolites II* (Ed. by J. Bertrand-Sarfati and C. Monty), pp. 193–226. Kluwer Academic Publishers, Dordrecht.

Causse, C., Ghaleb, B., Hillaire-Marcel, C., Casanova, J., Fournier, M., Rouchy, J.M. and Servant, M. (1995) New U–Th dates (TIMS) from algal bioherms of the 'Minchin' (Middle Wurm) and from stromatolites of the early 'Tauca' (Late Glacial) lacustrine phases of Bolivian Altiplano. *Terra Abstracts*, **7,** 267.

Cohen, A.S. and Thouin, C. (1987) Nearshore carbonate deposits in Lake Tanganyika. *Geology*, **15,** 414–418.

Dean, W.E. and Eggleston, J.R. (1975) Comparative anatomy of marine and freshwater algal reefs, Bermuda and central New-York. *Bull. Geol. Soc. Am.*, **86,** 665–676.

Dean, W.E. and Fouch, T.D. (1983) Lacustrine Environment. In: *Carbonate Depositional Environments* (Ed. by P. A. Scholle, D. G. Bebout and C. H. Moore), *Mem. Am. Ass. Petrol. Geol.*, **33,** 98–130.

Eggleston, J.R. and Dean, W.E. (1976) Freshwater stromatolitic bioherms in Green Lake, New-York. In: *Stromatolites* (Ed. by M. R. Walter), pp. 479–488. Elsevier Sci. Pub., Amsterdam.

Freytet, P. and Plaziat, J.C. (1965) Importance des constructions algaires dues à des Cyanophycées dans les formations continentales du Crétacé supérieur et de l'Eocène du Languedoc. *Bull. Soc. Géol. Fr.*, **VII**, 679–694.

Freytet, P. and Plaziat, J.C. (1982) Continental Carbonate Sedimentation and Pedogenesis – Late Cretaceous and Early Tertiary of Southern France. *Contrib. Sedimentol.*, **12,** 213.

Golubic, S. and Fisher, A.G. (1975) Ecology of calcareous nodules forming in Little Conestoga Creek near Lancaster, Pennsylvania. *Verh. Int. Verein. Limnol.*, **19,** 2315–2323.

Hastenrath, S. and Kutzbach, J. (1985) Late Pleistocene climate and water budget of the South American Altiplano. *Quat. Res.*, **24,** 249–256.

Jones, B. and Renaut, R.W. (1994) Crystal fabrics and microbiota in large pisoliths from Laguna Pastos Grandes, Bolivia. *Sedimentology*, **41,** 1171–1202.

Kempe, S., Kazmierczak, J., Landmann, G., Konuk, T., Reimer, A. and Lipp, A. (1991) Largest known microbialites discovered in Lake Van, Turkey. *Nature*, **349,** 605–608.

Moore, L., Knott, B. and Stanley, N. (1984) The stromatolites of Lake Clifton, Western Australia. Living Structures Representing the Origins of Life. *Search*, **14,** 11–12.

Osborne, R.H., Licari, G.R. and Link, M.H. (1982) Modern lake stromatolites, Walter Lake, Nevada. *Sediment. Geol.*, **32,** 39–61.

Pedley, M. (1992) Freshwater (phytoherm) reefs: the role of biofilms and their bearing on marine reef cementation. *Sediment. Geol.*, **79,** 255–274.

Pentecost, A. (1988) Observations on growth rates and calcium carbonate deposition in the green alga Gongrosira. *New. Phyto.*, **110,** 249–253.

Pentecost, A. (1991) Calcification Processes in Algae and Cyanobacteria. In: *Calcareous Algae and Stromatolites* (Ed. by R. Riding), pp. 3–20. Springer-Verlag, Berlin.

Riding, R. (1979) Origin and diagenesis of lacustrine algal bioherms at the margin of the Ries crater, Upper Miocene, southern Germany. *Sedimentology,* **26,** 645–680.

Risacher, F. (1978) Le cadre géochimique des bassins à évaporites des Andes boliviennes. *Cah. O.R.S.T.O.M.*, sér. Géol., **X**, 37–48.

Risacher, F. (1992) *Géochimie des bassins à évaporites de l'altiplano bolivien.* Thesis, University Louis Pasteur of Strasbourg.

Risacher, F. and Eugster, H.P. (1979) Holocene pisoliths and encrustations associated with spring-fed surface pools, Pastos Grandes, Bolivia. *Sedimentology,* **26,** 253–270.

Risacher, F. and Fritz, B. (1991) Quaternary geological evolution of the salars of Uyuni and Coipasa, central Altiplano, Bolivia. *Chem. Geol.,* **90,** 211–231.

Rondeau, B. (1990) Géochimie isotopique et géochronologie des stromatolites lacustres quaternaires de l'altiplano bolivien. *Mém. University of Québec, Montréal.*

Scholl, D.W. (1960) Pleistocene algal pinnacles at Searles lake, California. *J. sedim. Petrol.,* **30,** 414–431.

Scholl, D.W & Taft, W.H. (1964) Algae, contributors to the formation of calcareous tufa, Mono Lake, California. *J. sedim. Petrol.,* **34,** 309–319.

Servant, M. and Fontes, J.C. (1978) Les lacs quaternaires des hauts-plateaux des Andes boliviennes. Premières . interprétations paléoclimatiques. *Cah. O.R.S.T.O.M.*, sér. Géol., **X**, 9–24.

Servant, M., Fournier, M., Argollo, J., Servant-Vildary, S., Sylvestre, F., Wirrmann, D. and Ybert, J.P. (1995) La dernière transition glaciaire/interglaciaire des Andes tropicales sud (Bolivie) d'après l'étude des variations des niveaux lacustres et des fluctuations glaciaires. *C.R. Acad. Sci. Paris,* **320,** 729–736.

Servant-Vildary, S. (1978) Les diatomées des dépôts lacustres quaternaires de l'Altiplano bolivien. *Cah. ORSTOM, Sér. géol.,* **10,** 25–35.

Servant-Vildary, S. and Mello e Sousa, S.H. (1993) Paleohydrology of the Quaternary saline Lake Ballivian (southern Bolivian Altiplano) based on diatom studies. *Int. J. Salt Lakes Res.,* **2,** 69–85.

Smith, G.M. (1950) *The Fresh-Water Algae of the United States.* McGraw-Hill, New-York.

Sylvestre, F., Servant-Vildary, S., Fournier, M. and Servant, M. Lake levels in southern Bolivian Altiplano (19°–21°S.) during the late Glacial based on diatom studies. *Int. J. Salt Lake Res.*, in press.

Winsborough, B.M., Seeler, J.S., Golubic, S., Folk, R.L & Maguire, B., Jr. (1994) Recent fresh-water stromatolites, stromatolitic mats and oncoids from Northeastern Mexico. In: *Phanerozoic Stromatolites II* (Ed. by J. Bertrand-Sarfati and C. Monty), pp. 71–100. Kluwer Academic, Dordrecht.

Wirrmann, D. and Mourguiart, P. (1995) Late Quaternary spatio-temporal limnological variations in the Altiplano of Bolivia and Peru. *Quat. Res.,* **43,** 344–354.

Wood, K.G. (1975) Photosynthesis of *Cladophora* in relation to light, and CO_2 limitation; $CaCO_3$ precipitation. *Ecology,* **56,** 479–484.

Manuscript received 21 September 1995; revision accepted 11 March 1996.